Am J Cancer Res 2019;9(12):2634-2649
www.ajcr.us /ISSN:2156-6976/ajcr0103238

Original Article

Prognostic and therapeutic relevance of cathepsin B in pediatric acute myeloid leukemia

Garima Pandey[1], Sameer Bakhshi[2], Manoj Kumar[3], Bhaskar Thakur[4], Prerna Jain[1], Punit Kaur[3], Shyam S Chauhan[1]

[1]Department of Biochemistry, All India Institute of Medical Sciences, New Delhi, India; [2]Department of Medical Oncology, All India Institute of Medical Sciences, New Delhi, India; [3]Department of Biophysics, All India Institute of Medical Sciences, New Delhi, India; [4]Department of Biostatistics, All India Institute of Medical Sciences, New Delhi, India

Received October 7, 2019; Accepted October 18, 2019; Epub December 1, 2019; Published December 15, 2019

Abstract: AML, the second most common childhood leukemia is also one of the deadliest cancers. High mortality rate in AML is due to high incidence of relapse after complete remission with chemotherapy and inadequate prognostic assessment of patients. Moreover, there is dearth of therapeutic targets for treatment of this malignancy. Previous pilot study (n = 24) by our group revealed strong association between cathepsin B (CTSB) overexpression in peripheral blood mononuclear cells (PBMCs) and poor survival outcome in pediatric AML patients. To further explore the clinical utility and role of this protease in pediatric AML, we measured its enzymatic activity and mRNA expression in PBMCs as well as bone marrow mononuclear cells (BMMCs) of patients (n = 101) and PBMCs of healthy controls. Our results revealed elevated CTSB activity ($P < 0.01$) and overexpression of its mRNA ($P < 0.01$) in AML patients. Interestingly CTSB in BMMCs of patients emerged as an independent prognostic marker when compared with other known risk factors. Moreover, chemical inhibition of CTSB activity compromised survival, and induced apoptosis in an AML cell line THP-1. We further demonstrate the inhibition of CTSB activity by chemotherapeutic agent doxorubicin in these cells. Docking and simulation studies suggested the binding of doxorubicin to CTSB with higher affinity than its known specific inhibitor CA-074 Me, thereby indicating that cell death induced by this drug may at least partly be mediated by CTSB inhibition. CTSB, therefore, may serve as a prognostic marker and an attractive chemotherapeutic target in pediatric AML.

Keywords: Cathepsin B, pediatric AML, leukemia, mononuclear cells

Introduction

Acute leukemia is one of the most frequent hematological malignancies in children, of which 20% cases are of myeloid origin i.e., AML. Although intensification of chemotherapy, better supportive care and salvage therapy has improved the survival outcome of pediatric AML patients, there is no significant reduction in relapse and non-response rate [1]. However, further augmentation of current chemotherapy is unattainable due to treatment-related mortalities. Therefore, it is essential to identify newer molecular targets for development of better drugs for the treatment of pediatric AML. Risk factor assessment based on frequently occurring karyotypic alterations, and somatic mutations such as t(8,21), inv(16), t(15,17), and FLT3, NPM1, CEBPA respectively has assisted in deciding patient-specific treatment strategies [2-4]. Despite recent progress in diagnosis and therapy, the prognosis of this malignancy remains a challenge. Several proteases have been identified as potential biomarkers due to their deregulated expression in various cancers. CTSB is an endolysosomal cysteine protease and is of significant importance due to its involvement in several pathological and oncogenic processes [5-7]. In healthy cells, it is primarily involved in protein turnover and degradation with stringent regulation of its activity at multiple levels. However, this control is lost in malignant cells, thereby leading to its overexpression in a variety of solid tumors. The elevated activity/expression of CTSB contributes to tumor growth, invasion, and metastasis. Prognostic significance of this protease has been reported in tumors of the breast

[8], ovary [9], lung [10] and brain [11]. In a previous study, we demonstrated elevated activity/expression of CTSB and another lysosomal cysteine protease cathepsin L (CTSL) in a small cohort of pediatric AML patients [12]. We further established CTSL as an independent prognostic marker in this malignancy [13]. However, the clinical significance of CTSB in pediatric AML remained unclear.

Various *in-vivo* and *in-vitro* studies suggested the role of CTSB in conferring a survival advantage to cancer cells by promoting tumor cell proliferation [14]. In view of these reports specific chemical inhibitors of this protease and methods to silence/downregulate its expression have been developed. Inhibition of CTSB activity reduced tumor cell survival and growth in several cancers [15, 16]. However, no such information about its role in leukemic cells was available. Therefore, the present study was planned to assess the activity/expression of CTSB in mononuclear cells isolated from peripheral blood and bone marrow aspirate in a large cohort of 101 pediatric AML patients. In order to evaluate its utility to monitor the course of disease, the activity of this protease was also measured in AML patients after induction chemotherapy. We also investigated the significance of this protease as a prognostic marker in pediatric AML. Furthermore, the role of CTSB in conferring a survival advantage to leukemic cells was studied by its chemical inhibition in THP-1 cells.

Our results demonstrate significant overexpression of CTSB in pediatric AML patients as compared to their healthy siblings (controls). By Cox regression analysis it emerged as an independent prognostic marker. Moreover, inhibition of CTSB in THP-1 cells compromised cell survival and induced caspase-mediated apoptosis, thereby suggesting its role in conferring a survival advantage to AML cells. Additionally, we envisaged that doxorubicin/daunorubicin and cytosine arabinoside, two primary AML drugs may mediate cell death in AML by inhibition of CTSB. Our results from docking and simulation studies revealed high-affinity binding of doxorubicin into CTSB active site leading to inhibition of its activity. These findings confirm the involvement of CTSB in leukemic cell survival, thereby suggesting it to be a potential therapeutic target for the management of AML.

Methods

Study design

The present study was conducted at the All India Institute of Medical Sciences (AIIMS), New Delhi, India, after obtaining formal approval from the Institute's ethics committee [IESC/T-376/28.09.2012]. Prior informed consent was taken from legally accepted representatives of patients [13]. The study design is given in **Figure 1**.

Patients

A total of 106 pediatric AML patients attending medical oncology OPD at Dr. BRAIRCH, AIIMS, New Delhi, India were recruited for the present study. Both peripheral blood (PB, n = 101) and bone marrow aspirates (BM, n = 101) were taken from each patient. For some patients (n = 5) either PB or BM was not available. Bone marrow aspirates were collected during routine marrow analysis by a trained medical professional. Post Induction samples were collected after induction of patients with, cytosine arabinoside, and daunorubicin. Simultaneously, 35 age-matched healthy subjects were also included in this study to serve as controls.

Inclusion criteria: Newly diagnosed, previously untreated AML patients aged ≤ 18 years.

Exclusion criteria: Patients with myelodysplastic syndrome, previously known malignancy and acute promyelocytic leukemia.

Isolation of peripheral blood and bone marrow mononuclear cells

Peripheral blood and bone marrow aspirates were collected from pediatric AML patients in separate EDTA containing tubes. Ficoll density gradient centrifugation method was employed to isolate mononuclear cells from both peripheral blood and bone marrow aspirates. The mononuclear (opaque) layer was carefully transferred to a fresh Eppendorf tube, and contaminating RBCs were removed by lysis. Cell pellets thus obtained were stored at -80°C till further use.

CTSB enzyme assay

PBMCs and BMMCs were lysed in enzyme assay lysis buffer (50 mM Tris HCl, pH 6.8; 150 mM NaCl; 10% glycerol; 1% Nonidet P-40) by

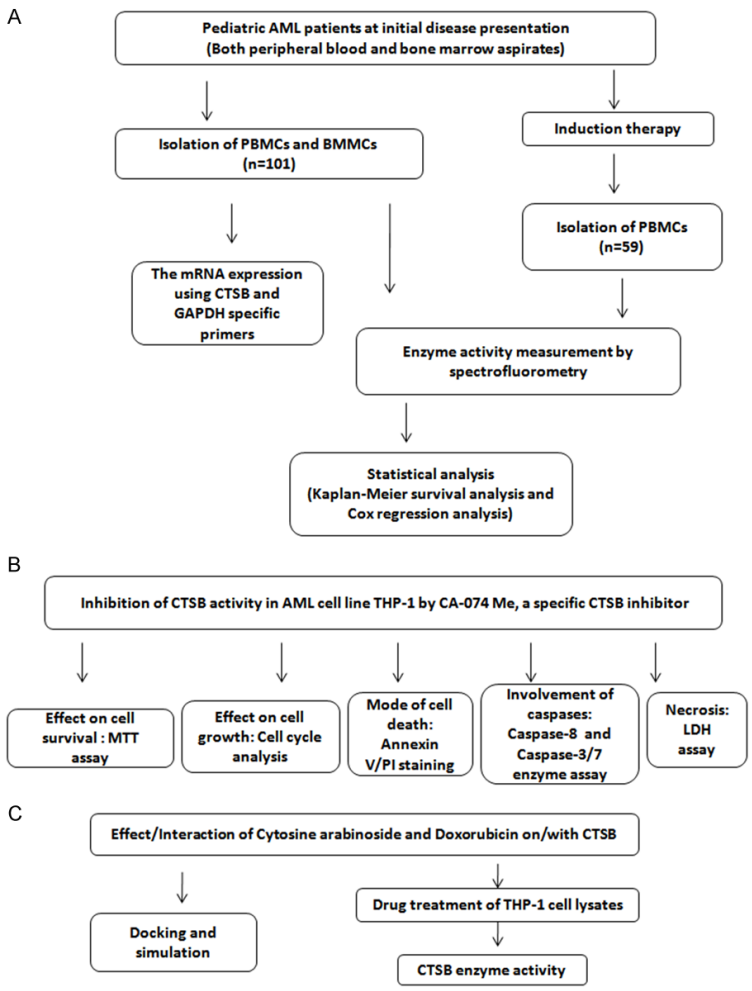

Figure 1. Schematic diagram depicting the study design. A. Patient samples were collected to determine CTSB expression levels at different time points. B. *In-vitro* experiments were carried out to evaluate the effects of CTSB inhibition on THP-1 cell survival. C. Docking and simulation studies were performed to identify the effect of commonly used AML drugs on CTSB.

two freeze-thaw cycles. Then the cell debris from the total lysate was removed by centrifugation at 5,000×g at 4°C for 10 minutes and clear lysate transferred to a fresh tube to be used for all estimations. Bicinchoninic acid assay method was employed for protein estimation in the lysate. An aliquot of lysate containing 50 µg of protein was used for assaying CTSB activity using CBZ-Phe-Arg-NMec, a fluorogenic synthetic substrate as described previously [12]. CTSB enzyme activity was expressed as RFU/min/mg protein (relative fluorescence units per minute per milligram protein).

Isolation of RNA and reverse transcription

Total cellular RNA (1 µg) isolated from PBMCs and BMMCs using TRIZOL Reagent BD™ (Sigma-Aldrich, St. Louis, MO, USA) according to manufacturer's protocol was reverse transcribed using random hexamers and RevertAid™ Reverse Transcriptase (MBI Fermentas, Vilnius, Lithuania). Real-time PCR using specific primers (IDT Technologies) for human CTSB or GAPDH was carried out as described earlier [12, 13]. The $2^{-\Delta Ct}$ method was employed for the calculation of Ct values.

Cell line and reagents

Human acute monocytic leukemia cell line, THP-1, was procured from NCCS, Pune, India and cultured in Roswell Park Memorial Institute (RPMI) 1640 medium (GIBCO-BRL, MD, USA), supplemented with 10% FBS and penicillin/streptomycin (100 µg/ml) (Sigma-Aldrich). The culture was maintained at 37°C in a humidified atmosphere containing 5% CO_2. CTSB inhibitor CA-074 Me [(L-3-*trans*-(Propylcarbamyl) oxirane-2-carbonyl)-L-isoleucyl-L-proline methyl ester] of greater than 99% purity was purchased from Sigma-Aldrich (St. Louis, MO, USA) and dissolved in ethanol.

Cell viability assay

THP-1 cells were seeded in a 96 well plate at a density of 5×10^3 cells per well and treated with different concentrations of CA074 Me. 5 mg/ml MTT solution was prepared by dissolving MTT dye in RPMI medium, and 10 µl of this solution was added to each well after 48 hours of CA-074 Me treatment. After 4 hours of incubation in MTT solution, 67.5 µL of solubilizing solution (1:1 ratio of dimethylformamide and 20% SDS) was added to each well to dissolve formazan crystals. Absorbance was measured using an ELISA plate reader at 570 nm. Cells treated with vehicle solution were processed identically and served as controls. Percentage of cell survival was calculated for each concentration of CA-074 Me with respect to vehicle treated cells.

Table 1. Summary of the baseline clinical characteristics of pediatric AML patients and healthy controls [13]

Source of blood	Patient characteristics median value (Range)				
	Age (years)	Gender ratio (M:F)	Hemoglobin (g/dl)	Total leukocyte count ($\times 10^3/\mu l$)	Platelet count ($\times 10^3/\mu l$)
AML patients Peripheral blood (n = 101) and bone marrow aspirate (n = 101)	10 (0.3-18)	2.1:1	7.8 (2.3-14.4)	20.1 (1.1-359.0)	29.5 (3.0-583.0)
Healthy controls Peripheral blood (n = 35)	10 (4-18)	1.05:1	9.5 (7.5-12.4)	5.9 (4.6-9)	210.5 (154.0-372.0)

Cell cycle analysis

Cells were cultured in serum-free media for 24 hours for synchronization of the cell cycle. Then 2×10^5 of these cells were seeded in each well of a six-well plate followed by treatment with 10 μM of CA-074 Me. After 48 hours, cells were washed with ice-cold PBS and fixed in ethanol (70% v/v) overnight at -20°C. Next day ethanol was removed by centrifugation and cells were washed twice with ice-cold PBS, stained with Propidium Iodide (PI) for 15 minutes at room temperature and subjected to FACS analysis. The distribution of cells in different phases of the cell cycle was analyzed by BD FACSDiva Software.

Apoptosis assay

Annexin V/PI staining assay was performed using the Annexin V apoptosis detection kit (BD Biosciences, San Jose, CA) according to the manufacturer's instructions. Briefly, 2×10^5 cells were seeded in each well of a six-well plate and treated with CTSB inhibitor. After incubating them for the indicated times, they were stained with FITC Annexin V and PI. Percentage of cells in early (Annexin V-FITC only) and late apoptotic phase (both Annexin V-FITC and PI) were quantitated using BD FACS-Diva software.

Caspase assay

Caspase activity was assayed using a Promega Kit (Madison WI, USA) according to the manufacturer's protocol. THP-1 cells (5×10^3) seeded in each well of a 96 well plate were treated with 10 μM CTSB inhibitor for the indicated time in a CO_2 incubator at 37°C. Then, 100 μl of Apo-Glo™ assay reagent was added to each well and incubated at 22°C for 1 hour. Luminescence was measured using Biotek ELISA reader (Winooski, VT, USA), and the caspase activity was expressed as RLU (relative luciferase units).

LDH assay

LDH assay (Nonradioactive cytotoxicity assay) measures cell death resulting from necrosis by detecting the release of a cytosolic enzyme, lactate dehydrogenase (LDH) upon cell lysis. THP-1 cells were treated with 10 μM CA-074 Me for 24 hours, and CytoTox 96 assay was performed according to the manufacturer's protocol (Promega, Madison WI USA). Cells treated with ethanol solution served as vehicle control. Maximum LDH release control wells contained cells treated with lysis solution for 45 minutes before the addition of LDH substrate and used for calculating percent cytotoxicity. After 24 hours of treatment, cells were centrifuged to remove any suspended debris, and 50 μl of LDH substrate was added to 50 μl of supernatant from each well. After an hour of incubation with the substrate, 50 μl of stop solution was added to the wells, and absorbance was recorded at 492 nm within an hour of adding stop solution.

Docking and simulation studies

Molecular modeling studies were performed to understand the potential mode of binding and get insights into the protein-ligand interactions between the various ligands (CA-074 Me, doxorubicin, and cytosine arabinoside) and human CTSB. The available 3D crystal structure of human cathepsin (PDB: 3AI8 A) [17] was taken as the receptor protein while the co-ordinates of CA-074 Me (PDB: 2DC9) [unpublished], doxorubicin (PDB: 4ZVM) [18] and cytosine arabinoside (PDB: 1P5Z) [19] were extracted from their respective co-crystal complexes. The protein atoms were prepared for docking studies by removing the co-crystallized ligand and solvent waters from the protein co-complex (PDB: 3AI8 A), assigned force field parameters CHARMm 33.1 [20, 21] and molecule subjected to energy minimization. The binding site for performing docking studies of ligands was defined in the prepared protein receptor around the active

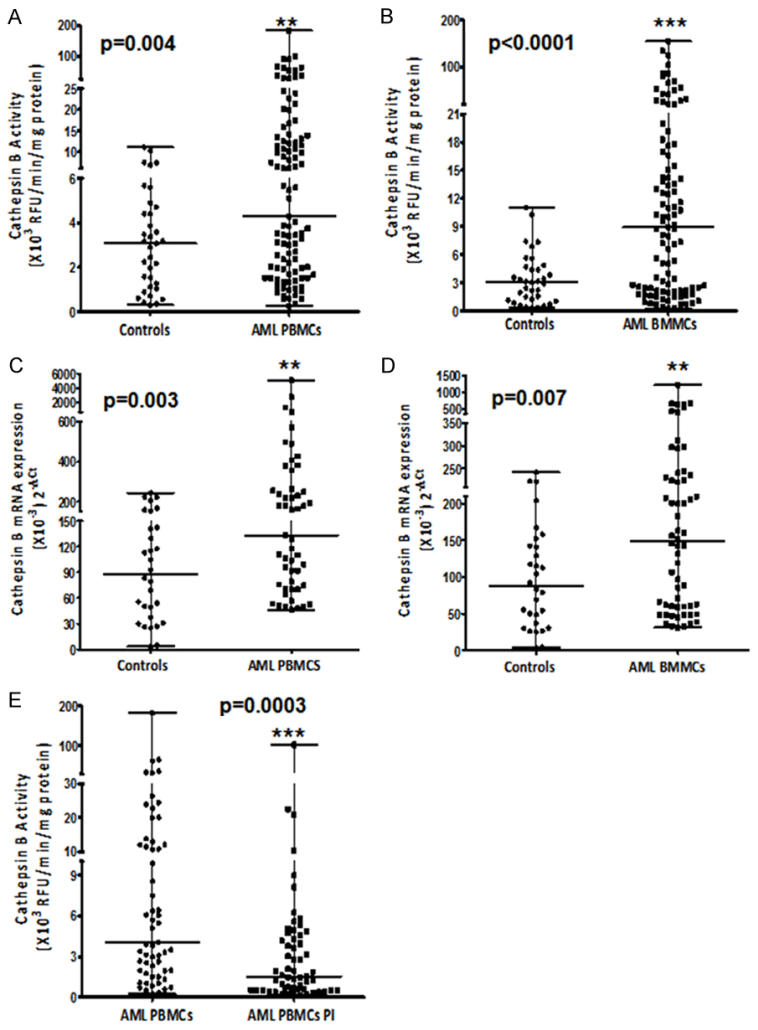

Figure 2. CTSB overexpression in pediatric AML patients. Dot plot of CTSB activity in, (A) PBMCs and, (B) BMMCs of patients (n = 101) compared to PBMCs of controls (n = 35) at initial presentation of the disease. PBMCs/BMMCs lysates containing equal amount of total proteins (50 µg) was used to assay CTSB activity using a synthetic fluorogenic substrate as described in materials and methods. Similarly, CTSB mRNA expression in, (C) PBMCs isolated from patients (n = 51) and healthy controls (n = 30) as well as in, (D) BMMCs isolated from patients (n = 60) was assessed by qRT-PCR using specific primers. Simultaneously, the expression of GAPDH was quantitated and used for normalization. Then the expression of CTSB mRNA in patients' PBMCs and BMMCs were individually compared to its expression in PBMCs of healthy controls. (E) CTSB activity before and after therapy was also assessed and compared in AML patients (n = 59). Each dot represents the activity or mRNA levels of an individual patient. Median values are represented by the horizontal line in the middle. Mann-Whitney U test and Wilcoxon matched-pairs signed-rank test was applied to test the statistical significance. $P < 0.05$ was considered statistically significant, and denoted by $^{**}p < 0.01$ and $^{***}p < 0.001$.

site residues. The selected side chains of residues at the binding site (Gln23, His110, His111, Phe174, His199, and Trp221) were treated as flexible during the docking procedure for an induced fit effect. Co-ordinates of each of the individual ligand extracted from their respective crystal complexes were also energy minimized using force field parameters. Each optimized ligand was individually docked into the defined binding site of human CTSB with the help of molecular docking program AutoDock 4.2.6 [22, 23] using default docking parameters (GA run - 10, population size - 150, rate of gene mutation - 0.02, rate of crossover - 0.8 and maximum number of evaluation - 25 million). 10 docked poses (positional conformers) from each independent docking run were clustered together if their docked position differed by less than 1.5 Å. The minimum binding energy of the docked pose from the largest cluster was taken as the most probable binding mode. The selected docked complex was energy minimized to remove steric clashes. The protein-ligand complex was further refined by molecular dynamics (MD) simulation for 10.2 ns using DESMOND [24] simulation engine to relax the protein atoms kept as rigid barring some selected side chains in the binding site which were treated as flexible during the docking process. This refined docked complex was analyzed to identify the potential binding mode and interactions between ligand and receptor.

Statistical analysis

In this study, statistical analysis was performed using Stata version 13.1 (StataCorp, College Station, TX, USA) and GraphPad Prism software (GraphPad software Inc., Version 5.0, La Jolla, CA, USA). For comparison between patients and controls, the Mann-Whitney U test or Wilcoxon matched-pairs signed-rank test was employed. Kaplan-Meier analysis was used for the evaluation of survival significance. Survival time was censored on December 31st, 2016, or at the last

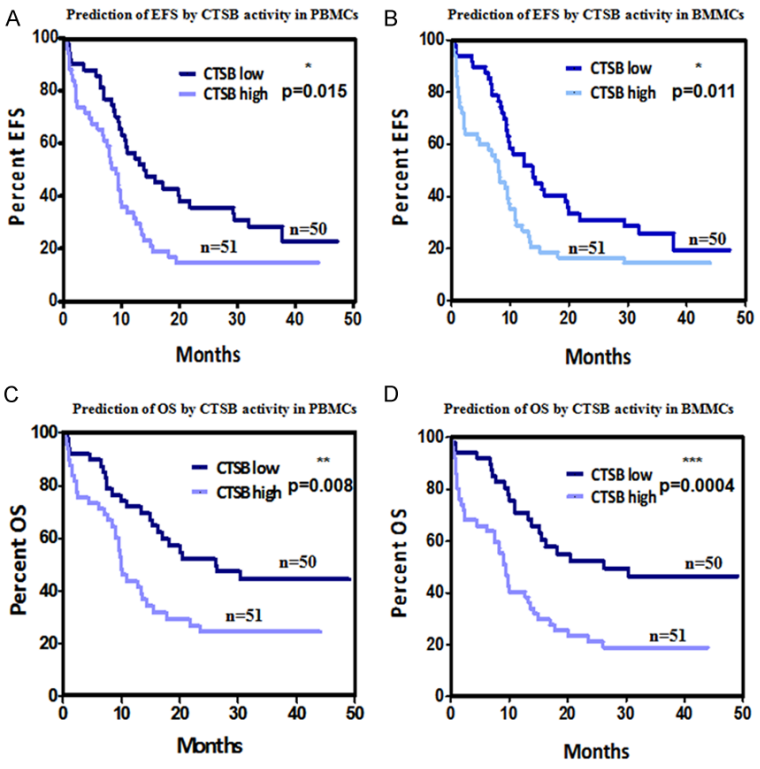

Figure 3. Impact of CTSB expression on survival of pediatric AML patients. A, B. Kaplan-Meier survival plots displaying the event-free survival (EFS) of the whole cohort based on CTSB activity in PBMCs and BMMCs, respectively. C, D. Kaplan-Meier survival plots exhibiting the overall survival (OS) of patients by CTSB activity in the two-types of mononuclear cells. The whole cohort was divided into two groups based on their median CTSB activity as low versus high. The log-rank test was used to calculate *p*-values. Survival curves significantly different from each other have been marked by *p < 0.05, **p < 0.01 and ***p < 0.001.

follow-up. Whereas event-free survival (EFS) was defined as the time between diagnosis and an event, which was either relapse or death; overall survival (OS) was considered as the time between diagnosis and death due to any cause. Survival was further estimated by fitting the data with a Cox regression model. Univariate and multivariate Cox regression analyses were performed with various clinical and cytogenetic patient characteristics. Factors which were found to be significant in univariate analysis (P < 0.1) served as candidates for multiple cox regression analysis. All tests were two-sided, and a P ≤ 0.05 was considered statistically significant.

Results

Elevated enzymatic activity and mRNA expression of CTSB in pediatric AML patients

Baseline clinical characteristics of pediatric AML patients (n = 101) and healthy controls (n = 35) are described previously [13] and summarized in **Table 1**.

The enzyme activity of CTSB in pediatric AML patients was assayed using a synthetic fluorogenic substrate in both PBMCs and BMMCs isolated from peripheral blood and bone marrow aspirates, respectively. Our results demonstrate a significant increase in CTSB activity in AML patients as compared to healthy controls. Specifically, CTSB activity was elevated by 1.4 and 2.9 fold in PBMCs (**Figure 2A**) and BMMCs (**Figure 2B**) of these patients respectively, as compared to PBMCs of healthy controls. Moreover, CTSB activity was found to be 1.9 fold higher in BMMCs than in PBMCs of these patients (graph not shown).

To quantify CTSB mRNA expression qRT-PCR was employed. Our results show a 1.52 fold increase in CTSB mRNA expression in PBMCs of AML patients as compared to healthy controls (**Figure 2C**). The CTSB mRNA levels in BMMCs of these patients were elevated by 1.7 fold than controls (**Figure 2D**, Mann-Whitney U test, P < 0.05).

We next sought to investigate CTSB activity in AML patients after induction chemotherapy. Post induction peripheral blood samples were available only from 59 patients out of 101 patients. We observed remission in 95% (56/59) of patients after the first round of therapy. Interestingly 71% (42/59) of them displayed a significant decrease in CTSB activity after induction chemotherapy (**Figure 2E**, Wilcoxon matched-pairs signed-rank test, P < 0.05).

Overexpression of CTSB as a predictor of poor event-free and overall survival of AML patients

Kaplan-Meier survival analysis was performed to determine the impact of CTSB overexpression on the progression and outcome of the disease. Patients were subdivided into two groups

Table 2. Survival analysis of pediatric AML patients on the basis of median CTSB activity

Parameter		CTSB activity PBMCs (low)	CTSB activity PBMCs (high)	*p*-value	CTSB activity BMMCs (low)	CTSB activity BMMCs (high)	*p*-value
EFS	Median EFS (Months)	14.3	8.23	0.015	13.8	8.2	0.011
OS	Median OS (Months)	26.2	9.8	0.008	26.2	9.5	0.0004

Table 3. Univariate and multivariate analysis of the effect of clinical, cytogenetic, PB and BM CTSB levels on event free survival (EFS) of pediatric AML patients

Univariate EFS				
		p-value	HR	95% CI
CTSB (PBMC)	High (n = 51)	0.017	1.76	(1.10-2.79)
	Low (n = 50)			
CTSB (BMMC)	High (n = 51)	0.013	2.03	(1.21-3.39)
	Low (n = 50)			
TLC (×10^3/μl)	> 20 (n = 54)	0.507	1.16	(0.75-1.81)
	< 20 (n = 52)			
Cytogenetics	Good (n = 25)	0.947	0.98	(0.54-1.77)
	Intermediate (n = 39)			
Cytogenetics	Good (n = 25)	0.867	0.75	(0.36-2.09)
	Poor (n = 10)			
AML1-ETO	Present (n = 31)	0.452	0.81	(0.48-1.39)
	Absent (n = 49)			
Age	> 10 (n = 53)	0.925	0.98	(0.63-1.53)
	< 10 (n = 53)			
Sex	Female (n = 34)	0.071	0.63	(0.39-1.04)
	Male (n = 72)			
Platelets (×10^3/μl)	> 50 (n = 29)	0.581	0.87	(0.54-1.42)
	< 50 (n = 77)			
Multivariate EFS				
		p-value	HR	95% CI
CTSB (BMMC)	High (n = 50)	0.071	1.64	(0.96-2.80)
	Low (n = 46)			
CTSB (PBMC)	High (n = 49)	0.254	1.36	(0.80-2.32)
	Low (n = 47)			
Sex	Female (n = 29)	0.176	0.69	(0.41-1.18)
	Male (n = 67)			

HR = hazard ratio, CI = confidence interval, n = number of patients, TLC = total leukocyte count, AML1-ETO = t(8,21) translocation.

based on their median CTSB values as, CTSB high and CTSB low. This analysis revealed significant differences in EFS and OS between CTSB high and low groups in both PBMCs and BMMCs (**Figure 3**; **Table 2**).

Cox regression analysis was performed to test if CTSB could serve as an independent prognostic marker. In Univariate analysis, CTSB in PBMCs (P = 0.017), as well as in BMMCs (P = 0.013) and sex of patients (P = 0.071) contributed significantly to the EFS (**Table 3**). However, only CTSB in PBMCs (P = 0.010) and BMMCs (P = 0.001), exhibited significant association with OS of AML patients (**Table 4**). Interestingly, in multivariate analysis, only CTSB in BMMCs displayed a prognostic impact on OS (P = 0.003, **Table 4**) and promising some amount of impact on EFS (p = 0.07) of pediatric AML patients. Thus our results establish the prognostic significance of CTSB independent of other known cytogenetic and clinic-pathological risk factors.

Compromised survival of leukemic cells on treatment with cell-permeable CTSB inhibitor

In view of our observation on poor disease free and overall survival of patients expressing high CTSB activity, it was of interest to investigate the role of this protease on survival and proliferation of leukemic cells. For this purpose THP-1 cells (a cell line derived from one-year-old infant suffering from AML) were treated with a cell-permeable specific inhibitor of CTSB and the effect of this treatment on the survival and growth of these cells was assessed.

As evident from **Figure 4A**, treatment of THP-1 cells with increasing concentrations of CA-074 Me resulted in a dose dependent inhibition of CTSB activity and 10 μM concentration of this inhibitor abolished 99% of CTSB activity. Similarly, treatment of THP-1 cells with CA-074 Me decreased the viability of these cells in a dose-dependent manner, and 10 μM concentration of this inhibitor reduced cell survival by approximately 60%. However, no such effect of vehicle solution on cell viability/CTSB activity was evi-

Table 4. Univariate and multivariate analysis of the effect of clinical, cytogenetic, PB and BM CTSB levels on overall survival (OS) of pediatric AML patients

Univariate OS				
		p-value	HR	95% CI
CTSB (PBMC)	High (n = 51)	0.010	1.99	(1.18-3.38)
	Low (n = 50)			
CTSB (BMMC)	High (n = 51)	0.001	2.49	(1.47-4.22)
	Low (n = 50)			
TLC (×10^3/μl)	> 20 (n = 54)	0.583	1.15	(0.70-1.88)
	< 20 (n = 52)			
Cytogenetics	Good (n = 25)	0.532	0.80	(0.40-1.60)
	Intermediate (n = 39)			
Cytogenetics	Good (n = 25)	0.422	0.61	(0.18-2.03)
	Poor (n = 10)			
AML1-ETO	Present (n = 31)	0.158	0.53	(0.27-1.02)
	Absent (n = 49)			
Age	> 10 (n = 53)	0.727	0.91	(0.55-1.50)
	< 10 (n = 53)			
Sex	Female (n = 34)	0.120	0.64	(0.37-1.22)
	Male (n = 72)			
Platelets (×10^3/μl)	> 50 (n = 29)	0.224	0.70	(0.39-1.24)
	< 50 (n = 77)			
Multivariate OS				
		p-value	HR	95% CI
CTSB (BMMC)	High (n = 50)	0.003	2.59	(1.40-4.80)
	Low (n = 46)			
CTSB (PBMC)	High (n = 49)	0.353	1.32	(0.73-2.38)
	Low (n = 47)			

HR = hazard ratio, CI = confidence interval, n = number of patients, TLC = total leukocyte count, AML1-ETO = t(8,21) translocation.

dent (**Figure 4B**). Thus our results demonstrate a parallel decrease in CTSB activity and cell viability with increasing concentrations of CTSB inhibitor, thereby suggesting the role of this protease in AML cell survival.

Interestingly, treatment of THP-1 cells with CTSB inhibitor exhibited a dramatic effect on the distribution of cells in different phases of the cell cycle. Analysis of DNA histogram obtained after subjecting PI stained samples to flow cytometry revealed a dramatic increase in the number of cells in the sub-G0 phase of the cell cycle on treatment with CA074 Me as compared to untreated cells (**Figure 4C**). This was accompanied by a simultaneous decrease in the number of cells in S and G2/M phase. These results suggest that inhibition of CTSB reduces proliferation and induces death of THP-1 cells.

CTSB inhibition induces apoptosis in THP-1 cells by activation of caspases

To elucidate the mechanism of cell death induced by CTSB inhibition, CA-074 Me treated THP-1 cells (for 24 or 48 hours) were subjected to Annexin V/PI staining followed by flow cytometric analysis. After 24 hours of treatment, a significant increase in the number of both early (0.5%) and late apoptotic (34%) cells was observed as compared to control cells (0.15% and 3.1% respectively) (**Figure 5A**). However, after 48 hours of the CA-074 Me treatment, we found a significant increase in the number of only late apoptotic cells (**Figure 5B**). These results demonstrate the induction of apoptosis in AML cells by CTSB inhibition. Caspase activity was assayed in these cells to assess its involvement in CA-074 Me induced apoptosis of THP-1 cells, and the results are presented in **Figure 6**. As evident from these results, CTSB inhibition lead to a significant increase in caspase 8 and caspase 3/7 activity (**Figure 6A-C** respectively). Therefore from these results, we conclude that apoptosis mediated by CTSB inhibition in leukemic cells is caspase-dependent.

We next investigated the contribution of necrosis in CA-074 Me mediated cell death in AML. LDH assay (Nonradioactive cytotoxicity assay) was used to measure cell death resulting from necrosis. The assay measured the release of cytosolic enzyme lactate dehydrogenase (LDH) upon cell lysis and was performed as mentioned in materials and methods. After 24 hours of CA-074 Me treatment, no significant difference in LDH release was observed between treated and untreated THP-1 cells (**Figure 6D**).

Modeling of CTSB with doxorubicin and cytosine arabinoside: docking and simulation studies

Our results so far demonstrate CTSB inhibition as one mode of inducing cell death in AML cells,

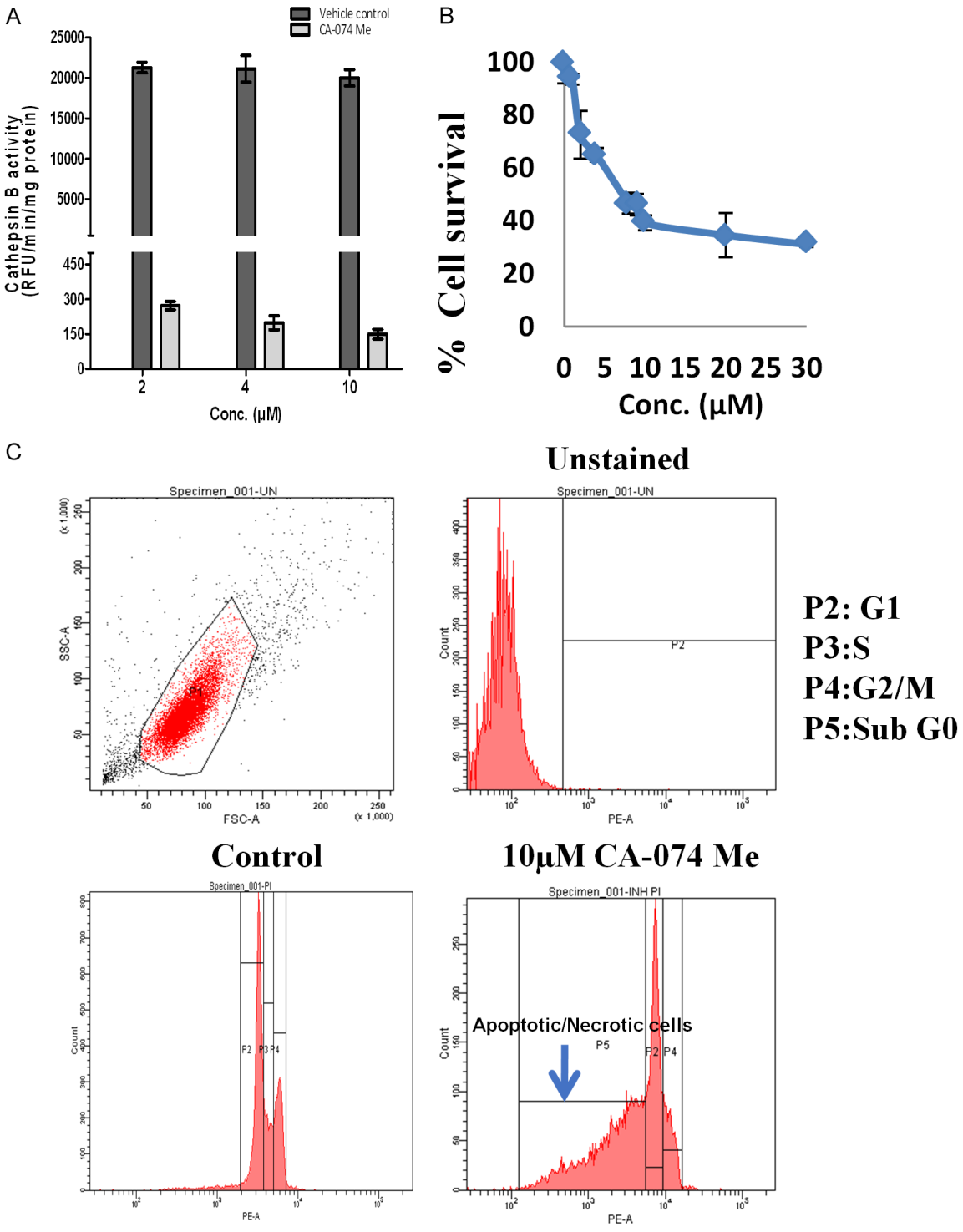

Figure 4. Effect of CTSB inhibition on AML cell survival and growth. A. Inhibition of CTSB activity in THP-1 cells by CA-074 Me. THP-1 cells treated for 48 hours with varying concentrations of CA-074 Me were washed and lysed with enzyme assay lysis buffer. The activity of CTSB in the cell lysate was assessed using a synthetic substrate as described earlier. Cells treated with ethanol were processed identically and served as controls. The activity of CTSB in treated and untreated cells was compared. Cells treated with ethanol solution were processed similarly and served as vehicle control. B. Effect of CTSB inhibition on AML cell viability. THP-1 cells treated for 48 hours with varying concentrations of CA-074 Me (0-30 μM) or vehicle solution were subjected to MTT assay. Vehicle treated cells were considered to be 100% viable, and % viability for each concentration was calculated with respect to these cells. C. Cell cycle analysis of THP-1 cells in the absence and presence of CTSB inhibitor. Cells after treatment with CA-

074 Me (10 μM)/vehicle solution for 48 hours were fixed in ethanol, permeabilized with Triton X-100 and stained with PI. Then these cells were subjected to flow cytometric analysis. About 10,000 events were acquired in BD FACSCantoTM flow cytometer. The analysis was performed using BD FACS diva software. Analysis of DNA content shows a significantly higher number of cells in the sub G0 phase of the cell cycle on CTSB inhibition as compared to vehicle-treated controls. All experiments were performed in triplicates.

thereby suggesting it to be a potential therapeutic target for treating this disease. We next envisaged if currently used AML drugs affect CTSB in achieving their anticancer effects. We studied the potential binding interactions, if any, between cytosine arabinoside/doxorubicin and CTSB.

The modeled and docked binding mode of CA-074 Me with human CTSB was similar to the reported co-crystal conformation of CA-074 Me with bovine CTSB (PDB: 2DC9). The bound compound was fairly stable throughout the simulation and the receptor-ligand interactions comprised predominantly van der Waals interactions in addition to the two hydrogen bonds (**Figure 7A**). This was clearly reflected by a more pronounced contribution from van der Waals interaction energy as compared to electrostatic interaction energy (**Table 5**). The non-polar propyl moiety of the ligand was seen to interact with the residues Pro76, Ala173 and Ala200 while isoleucyl moiety of the ligand interacted with Val176, Met196 and Trp221 through van der Waals interactions. Hydrogen bonds formed between the ligand and side chain of Gln23 and main chain of Gly198 contributed majorly in stabilizing the ligand which was retained in the binding pocket during MD simulation.

During the docking procedure, the side-chain conformations of residues in the binding pocket were treated as flexible. This facilitated the binding of the bulky aromatic rings of doxorubicin, which could induce a conformational change in the orientation of the side chains. The planar aromatic moiety of doxorubicin was seen to be sandwiched between the aromatic rings of His198 and Trp221 (**Figure 7B**). One phenyl ring of doxorubicin formed stacking aromatic interaction with His198 while the other phenyl ring had the edge to face aromatic interaction with Trp221. The stacking interactions were optimized during MD simulation, as this resulted in a parallel stacking of aromatic rings to each other. Similarly, simulations resulted in optimization of the edge to face interaction as the Trp221 side chain was observed to be facing the aromatic ring of doxorubicin. The aromatic moiety of doxorubicin in the binding pocket occupied a position similar to nitroxoline, an aromatic ring containing an inhibitor of human CTSB (PDB: 3AI8) [17]. This bulky aromatic moiety of doxorubicin was further stabilized by hydrogen-bonded interactions between two oxygen atoms on the central aromatic ring with the side chain of Gln23 and His110. The hydroxyacetyl moiety on cyclohexane ring formed hydrogen bonds with the main chain nitrogen atoms of Cys26 and Glu122 while the position of oxanyl ring was held steady by hydrogen-bonded interactions between its hydroxyl and amino substituent and the main chain of Cys119 and side chain of His110 of the protein, respectively.

The compound, cytosine arabinoside docked into the binding pocket, but the resultant interactions with the protein atoms were not retained during MD simulations indicating that the docking was not stable. Although the cytosine ring of cytosine arabinoside was close to His199, it could not make stable stacking interaction. Moreover, the initial hydrogen bonds observed in the docked complex between hydroxyl and amino group of cytosine arabinoside and residues Gly24, Cys26, and Gly196 were disrupted during MD simulation. After MD simulation, the molecule cytosine arabinoside was seen to have moved away from the binding pocket.

To further confirm these results *in-vitro,* we treated THP-1 cell lysates with doxorubicin. Interestingly, a significant reduction in CTSB activity was observed in these cells on treatment with doxorubicin thereby validating our docking and simulation findings (**Figure 7C**, **7D**).

Discussion

Previously we demonstrated overexpression of CTSB in the PBMCs of a small cohort of 24 pediatric AML patients [12]. The main objective of the present study was to validate these find-

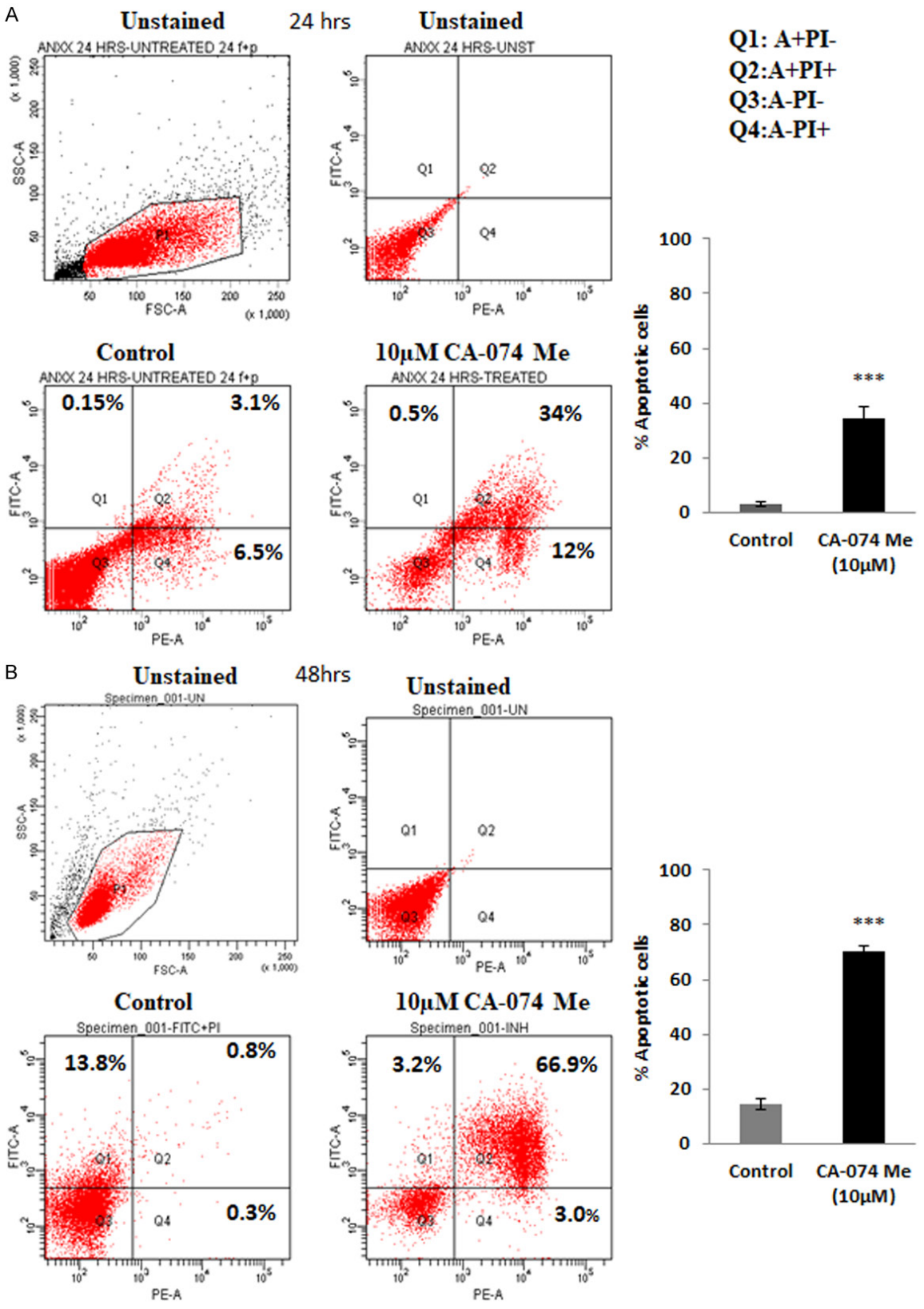

Figure 5. CTSB inhibition induces apoptosis in AML cells. Annexin V/PI assay was performed on THP-1 cells treated with CA-074 Me (10 µM) and assessed by flow cytometry. Representative biparametric histograms shown on the left depicting normal (Q3), early apoptotic (Q1), apoptotic (Q2) and necrotic (Q4) population of cells after, (A) 24 hours

and, (B) 48 hours of CTSB inhibition. The bar chart on the right represents the total apoptotic cell fraction (early plus late apoptotic) in CTSB inhibited and control cells. Results were statistically analyzed by two-tailed unpaired t-test and values significantly different ($p < 0.001$) from controls have been marked by ***.

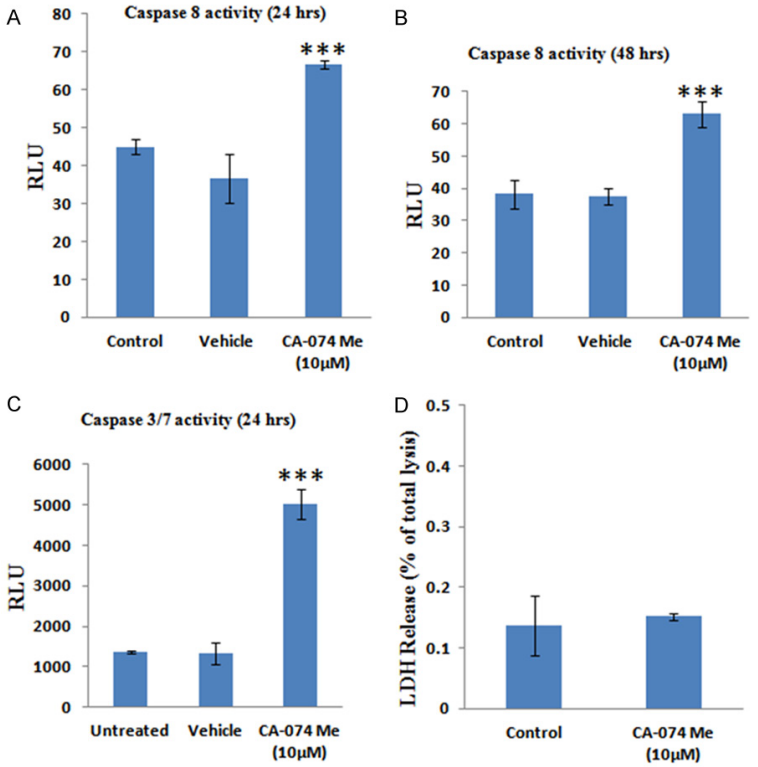

Figure 6. Involvement of caspases in CTSB inhibition induced apoptosis of THP-1 cells. (A, B) Caspase-8 and, (C) caspase-3/7 activity in THP-1 cells after treatment with CA-074 Me for indicated times was assayed using specific Apo-Glo™ assay reagent and compared with their activity in untreated as well as vehicle-treated cells. (D) Similarly, LDH release in THP-1 cells after abovementioned treatment for 24 hours was also assayed as described in materials and methods. Caspase activities have been represented in relative luciferase units (RLU). Values expressed are mean ± SD of three independent experiments performed in triplicate. Statistical significance was determined by unpaired t-test. Values significantly different from controls have been marked by ***$p < 0.001$.

of our pilot study in a large cohort of AML patients. Furthermore, in this study, for the first time, we demonstrate significantly higher expression of this protease in the BMMCs of these patients as compared to controls. Kaplan-Meier survival analysis revealed a strong association of increased CTSB activity with poor event-free and overall survival of these patients. Overexpression of CTSB has also been previously reported to predict poor patient survival outcomes in several cancers [25-27]. By univariate and multivariate Cox regression analysis, CTSB activity in BMMCs emerged as an independent prognostic marker in pediatric AML.

CTSB promotes the proliferation of hepatic stellate cells and therefore, has been proposed as a potential therapeutic target in this malignancy [28]. Interestingly, drugs induced release of CTSB from lysosomes results in the activation of the inflammasome and concomitant secretion of IL-1β, IL-17 leading to enhanced tumor growth of myeloid-derived suppressor cells [29]. Thus the role CTSB in cell proliferation and tumor growth has been extensively documented in solid tumors [30-34]. Only a single such study was carried out in leukemia and lymphoma cell lines where a general inhibitor of all cysteine cathepsins induced apoptosis in these cells [35]. However, this study did not investigate the role of individual cysteine cathepsins in this process. Thus, in view of this report and our observation on overexpression of CTSB in the active stage of AML, it was of interest to study the role of this protease in the survival of leukemia cells by using its specific inhibitor, CA-074 Me. Interestingly our results demonstrate that like other tumors, AML derived cells also undergo

ings in a larger cohort of patients and assess the prognostic relevance of CTSB and its utility as a therapeutic target in this disease. To achieve these objectives, we evaluated the activity and mRNA expression of this protease in pediatric AML patients at two-time points, i.e., at initial disease presentation and post-induction. We observed significantly higher CTSB activity and mRNA expression in both PBMCs and BMMCs of AML patients at disease diagnosis as compared to PBMCs of healthy controls. The expression of this protease exhibited a parallel decrease with remission of malignancy after induction chemotherapy. Thus results of the present study confirm the findings

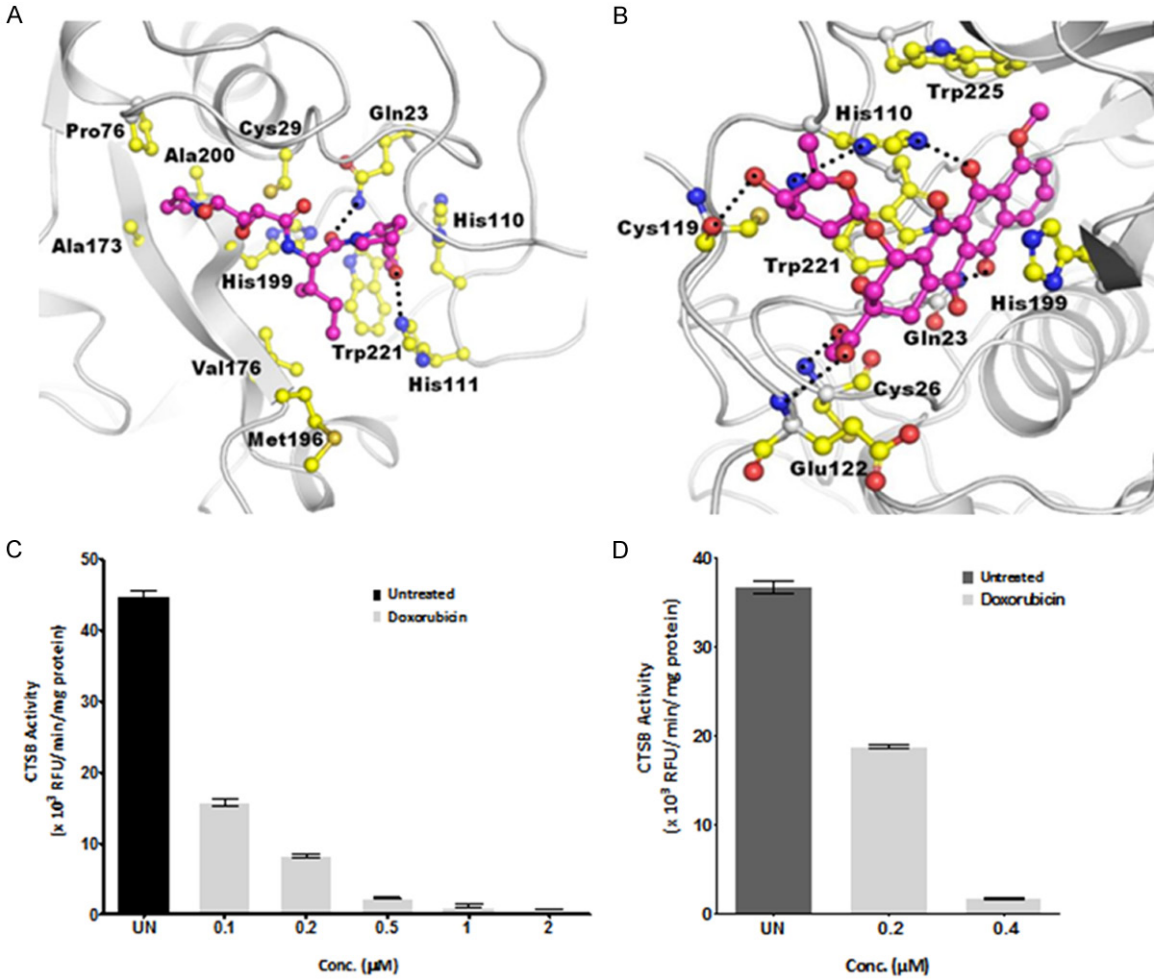

Figure 7. CTSB inhibition by AML drug, doxorubicin in THP-1 cells. (A) The interactions observed between human CTSB (grey, cartoon) and CA-074 Me (known inhibitor) (magenta, ball-and-stick) and, (B) between CTSB and doxorubicin (magenta, ball-and-stick). The planar aromatic moieties of doxorubicin are sandwiched between the aromatic rings of His198 and Trp221. Hydrogen-bonded interactions (black dotted lines) are indicated between CA074 Me/doxorubicin and protein residues. (C) THP-1 cells were lysed in enzyme assay lysis buffer and an aliquot of 50 μg of total protein was taken. Following treatment of the lysates with increasing concentrations of doxorubicin, CTSB enzyme activity was measured as described in material and methods. Untreated controls were processed similarly for comparison. (D) THP-1 cells in culture were treated with doxorubicin. After 48 hours of incubation at 37°C in 5% CO_2, cell pellets were collected, lysed and processed for measurement of CTSB enzyme activity.

Table 5. Calculated interaction energy between ligand and human cathepsin using CHARMm force field

Ligand	Forcefield	Total Interaction Energy (kcal/mol)	vdW Interaction Energy (kcal/mol)	Electrostatic Interaction Energy (kcal/mol)	Contacting residues (upto 4Å) Hydrogen bonded residues are shown in bold
CA-074 Me	CHARMm	-70.15	-45.59	-24.56	**Gln23**, Cys29, Pro76, His110, **His111**, Val176, Met196, **Gly198**, His199, Ala200 & Trp221
Doxorubicin	CHARMm	-85.11	-51.32	-33.79	**Gln23**, Ser25, **Cys26**, Cys29, Glu109, **His110**, **Cys119**, Glu122, Phe180, Leu181, His199, Ile201, Asn219, Trp221 & Trp225

apoptosis after CTSB inhibition. Previously, inhibition and/or knockdown of cathepsin B, D, and L has been shown to specifically trigger caspase-dependent apoptotic cell death in pancreatic β cells [36] and prostate cancer cells [37]. Similarly, downregulation of CTSB and uPAR

induced cytochrome-C mediated apoptosis in glioblastoma cells [38]. Consistent with these reports, inhibition of CTSB activity resulted in reduced survival and growth of AML cells. MTT assay revealed 40% cell survival on the treatment of THP-1 cells with CA-074 Me. Similarly, flow cytometric analysis demonstrated apoptosis/necrosis of more than 50% cells after inhibition of CTSB activity, thereby suggesting the therapeutic utility of this protease in AML. Caspase-8 is a key initiator of the extrinsic/receptor-mediated apoptotic pathway, whereas Caspase-3/7 is the final executioner of apoptosis activated by both intrinsic and extrinsic pathways and is itself activated by caspase-8. In line with reports on solid tumors [36-38], chemical inhibition of CTSB in AML cells induced activity/expression of caspases-3/7 and caspase-8. Thus, our results conclusively demonstrate caspase-dependent apoptosis of AML cells following CTSB inhibition.

The treatment of AML involves induction therapy by two most commonly used drugs cytosine arabinoside and an anthracycline, daunorubicin/doxorubicin. We predicted direct binding of doxorubicin to CTSB by the detailed analysis of the docked and simulated three-dimensional protein complexes. This analysis provides a detailed understanding of the ligand preferences, their interactions with the protein, and an assessment of the binding affinity of the ligand for the protein. The total interaction energy determined for the docked doxorubicin was found to be more favorable (negative) than CA-074 Me indicating its stronger binding to CTSB (**Table 5**). The better affinity of doxorubicin for human CTSB is majorly due to contribution from strong stacking interaction between the protein and ligand in addition to van der Waals interactions and hydrogen bonds. CA-074 Me formed van der Waals interaction but lacked stacking aromatic interactions. Crystal structures of human CTSB complexed with inhibitors (PDB: 3AI8, 1GMY, 4DMY & 1CSB) revealed the involvement of Gln23 in hydrogen-bonded contacts with each inhibitor, including CA-074 Me. Doxorubicin was also found to form hydrogen-bonded interaction with Gln23 in this modeled complex. The molecule cytosine arabinoside could not be retained in the binding pocket of human CTSB due to lack of stacking interaction with its aromatic cytosine ring or insufficient favorable van der Waals interaction to hold its non-polar component. This absence of adequate, stable interactions displaced it out of binding pocket during MD simulation. This analysis suggests doxorubicin as a CTSB inhibitor with a binding affinity greater than the well-known CTSB inhibitor CA-074 Me. To validate this, we treated THP-1 cells with doxorubicin for 48 hours followed by CTSB assay and observed a dose-dependent reduction in CTSB activity. Specifically, with 0.2 and 0.4 μM doxorubicin, this decrease was 2 and 17 fold respectively. Our results also displayed a dose-dependent effect of doxorubicin on CTSB activity in THP-1 cell lysates. Thus these results demonstrate that doxorubicin at least in part mediates its cytotoxic effects on leukemic cells through inhibition of CTSB.

In summary, our study reports CTSB overexpression and its significance as an independent predictor of survival outcome in pediatric AML patients. Moreover, inhibition of CTSB activity induces apoptosis in AML cells suggesting the contribution of this protease in the pathogenesis of this malignancy. We further show that commonly used chemotherapeutic doxorubicin directly binds to CTSB and inhibits its activity, indicating that doxorubicin may induce cell death in cancer cells partly via inhibition of CTSB activity.

Thus, our study, for the first time demonstrates the utility of CTSB as a potential therapeutic target in AML. Future studies may aim towards the development of specific CTSB inhibitors and also, testing the efficacy of targeting CTSB in animal models of leukemia.

Acknowledgements

GP received senior research fellowship (SRF) from the Council of Scientific and Industrial Research (CSIR), India and Institute fellowship from AIIMS.

Disclosure of conflict of interest

None.

Address correspondence to: Shyam S Chauhan, Department of Biochemistry, All India Institute of Medical Sciences, New Delhi, India. E-mail: s_s_chauhan@hotmail.com

References

[1] Rasche M, Zimmermann M, Borschel L, Bourquin JP, Dworzak M, Klingebiel T, Lehrn-

becher T, Creutzig U, Klusmann JH and Reinhardt D. Successes and challenges in the treatment of pediatric acute myeloid leukemia: a retrospective analysis of the AML-BFM trials from 1987 to 2012. Leukemia 2018; 32: 2167-2177.

[2] Tsukimoto I, Tawa A, Horibe K, Tabuchi K, Kigasawa H, Tsuchida M, Yabe H, Nakayama H, Kudo K, Kobayashi R, Hamamoto K, Imaizumi M, Morimoto A, Tsuchiya S and Hanada R. Risk-stratified therapy and the intensive use of cytarabine improves the outcome in childhood acute myeloid leukemia: the AML99 trial from the Japanese Childhood AML Cooperative Study Group. J Clin Oncol 2009; 27: 4007-4013.

[3] Pui CH, Carroll WL, Meshinchi S and Arceci RJ. Biology, risk stratification, and therapy of pediatric acute leukemias: an update. J Clin Oncol 2011; 29: 551-65.

[4] Zwaan CM, Kolb EA, Reinhardt D, Abrahamsson J, Adachi S, Aplenc R, De Bont ES, De Moerloose B, Dworzak M, Gibson BE, Hasle H, Leverger G, Locatelli F, Ragu C, Ribeiro RC, Rizzari C, Rubnitz JE, Smith OP, Sung L, Tomizawa D, van den Heuvel-Eibrink MM, Creutzig U and Kaspers GJ. Collaborative efforts driving progress in pediatric acute myeloid leukemia. J Clin Oncol 2015; 33: 2949-62.

[5] Aggarwal N and Sloane BF. Cathepsin B: multiple roles in cancer. Proteomics Clin Appl 2014; 8: 427-437.

[6] Manchanda M, Das P, Gahlot GPS, Singh R, Roeb E, Roderfeld M, Datta Gupta S, Saraya A, Pandey RM and Chauhan SS. Cathepsin L and B as potential markers for liver fibrosis: insights from patients and experimental models. Clin Transl Gastroenterol 2017; 8: e99.

[7] Mehra S, Kumar M, Manchanda M, Singh R, Thakur B, Rani N, Arava S, Narang R, Arya DS and Chauhan SS. Clinical significance of cathepsin L and cathepsin B in dilated cardiomyopathy. Mol Cell Biochem 2017; 428: 139-147.

[8] Nouh MA, Mohamed MM, El-Shinawi M, Shaalan MA, Cavallo-Medved D, Khaled HM and Sloane BF. Cathepsin B: a potential prognostic marker for inflammatory breast cancer. J Transl Med 2011; 9: 1.

[9] Scorilas A, Fotiou S, Tsiambas E, Yotis J, Kotsiandri F, Sameni M, Sloane BF and Talieri M. Determination of cathepsin B expression may offer additional prognostic information for ovarian cancer patients. Biol Chem 2002; 383: 1297-1303.

[10] Werle B, Lötterle H, Schanzenbächer U, Lah TT, Kalman E, Kayser K, Bülzebruck H, Schirren J, Krasovec M, Kos J and Spiess E. Immunochemical analysis of cathepsin B in lung tumours: an independent prognostic factor for squamous cell carcinoma patients. Br J Cancer 1999; 81: 510-9.

[11] Strojnik T, Kos J, Židanik B, Golouh R and Lah T. Cathepsin B immunohistochemical staining in tumor and endothelial cells is a new prognostic factor for survival in patients with brain tumors. Clin Cancer Res 1999; 5: 559-567.

[12] Jain M, Bakhshi S, Shukla AA and Chauhan SS. Cathepsins B and L in peripheral blood mononuclear cells of pediatric acute myeloid leukemia: potential poor prognostic markers. Ann Hematol 2010; 89: 1223-1232.

[13] Pandey G, Bakhshi S, Thakur B, Jain P and Chauhan SS. Prognostic significance of cathepsin L expression in pediatric acute myeloid leukemia. Leuk Lymphoma 2018; 59: 2175-2187.

[14] Vasiljeva O, Korovin M, Gajda M, Brodoefel H, Bojic L, Krüger A, Schurigt U, Sevenich L, Turk B, Peters C and Reinheckel T. Reduced tumour cell proliferation and delayed development of high-grade mammary carcinomas in cathepsin B-deficient mice. Oncogene 2008; 27: 4191-9.

[15] Ruan H, Hao S, Young P and Zhang H. Targeting cathepsin B for cancer therapies. Horiz Cancer Res 2015; 56: 23-40.

[16] Gondi CS and Rao JS. Cathepsin B as a cancer target. Expert Opin Ther Targets 2013; 17: 281-291.

[17] Mirković B, Renko M, Turk S, Sosič I, Jevnikar Z, Obermajer N, Turk D, Gobec S and Kos J. Novel mechanism of cathepsin B inhibition by antibiotic nitroxoline and related compounds. ChemMedChem 2011; 6: 1351-1356.

[18] Leung KK and Shilton BH. Binding of DNA-intercalating agents to oxidized and reduced quinone reductase 2. Biochemistry 2015; 54: 7438-7448.

[19] Sabini E, Ort S, Monnerjahn C, Konrad M and Lavie A. Structure of human dCK suggests strategies to improve anticancer and antiviral therapy. Nat Struct Biol 2003; 10: 513-9.

[20] Brooks BR, Bruccoleri RE, Olafson BD, States DJ, Swaminathan S and Karplus M. CHARMM: a program for macromolecular energy, minimization, and dynamics calculations. J Comput Chem 1983; 4: 187-217.

[21] Momany FA and Rone R. Validation of the general purpose QUANTA® 3.2/CHARMm® force field. J Comput Chem 1992; 13: 888-900.

[22] Morris GM, Goodsell DS, Halliday RS, Huey R, Hart WE, Belew RK and Olson AJ. Automated docking using a Lamarckian genetic algorithm and an empirical binding free energy function. J Comput Chem 1998; 19: 1639-1662.

[23] Morris GM, Huey R, Lindstrom W, Sanner MF, Belew RK, Goodsell DS and Olson AJ. AutoDock4 and AutoDockTools4: automated docking with selective receptor flexibility. J Comput Chem 2009; 30: 2785-2791.

[24] Bowers KJ, Chow DE, Xu H, et al. Scalable algorithms for molecular dynamics simulations on commodity clusters. SC 2006 conference, proceedings of the ACM/IEEE: IEEE 2006: 43.
[25] Ruan J, Zheng H, Rong X, Rong X, Zhang J, Fang W, Zhao P and Luo R. Over-expression of cathepsin B in hepatocellular carcinomas predicts poor prognosis of HCC patients. Mol Cancer 2016; 15: 17.
[26] Lah TT, Cercek M, Blejec A, Kos J, Gorodetsky E, Somers R and Daskal I. Cathepsin B, a prognostic indicator in lymph node-negative breast carcinoma patients: comparison with cathepsin D, cathepsin L, and other clinical indicators. Clin Cancer Res 2000; 6: 578-584.
[27] Gong F, Peng X, Luo C, Shen G, Zhao C, Zou L, Li L, Sang Y, Zhao Y and Zhao X. Cathepsin B as a potential prognostic and therapeutic marker for human lung squamous cell carcinoma. Mol Cancer 2013; 12: 125.
[28] Moles A, Tarrats N, Fernández-Checa JC and Marí M. Cathepsins B and D drive hepatic stellate cell proliferation and promote their fibrogenic potential. Hepatology 2009; 49: 1297-1307.
[29] Bruchard M, Mignot G, Derangère V, Chalmin F, Chevriaux A, Végran F, Boireau W, Simon B, Ryffel B, Connat JL, Kanellopoulos J, Martin F, Rébé C, Apetoh L and Ghiringhelli F. Chemotherapy-triggered cathepsin B release in myeloid-derived suppressor cells activates the Nlrp3 inflammasome and promotes tumor growth. Nat Med 2013; 19: 57-64.
[30] Bian B, Mongrain S, Cagnol S, Langlois MJ, Boulanger J, Bernatchez G, Carrier JC, Boudreau F and Rivard N. Cathepsin B promotes colorectal tumorigenesis, cell invasion, and metastasis. Mol Carcinog 2016; 55: 671-687.
[31] Mohanam S, Jasti SL, Kondraganti SR, Chandrasekar N, Lakka SS, Kin Y, Fuller GN, Yung AW, Kyritsis AP, Dinh DH, Olivero WC, Gujrati M, Ali-Osman F and Rao JS. Down-regulation of cathepsin B expression impairs the invasive and tumorigenic potential of human glioblastoma cells. Oncogene 2001; 20: 3665-73.
[32] Bengsch F, Buck A, Günther SC, Seiz JR, Tacke M, Pfeifer D, von Elverfeldt D, Sevenich L, Hillebrand LE, Kern U, Sameni M, Peters C, Sloane BF and Reinheckel T. Cell type-dependent pathogenic functions of overexpressed human cathepsin B in murine breast cancer progression. Oncogene 2014; 33: 4474-84.
[33] Tummalapalli P, Spomar D, Gondi CS, Olivero WC, Gujrati M, Dinh DH and Rao JS. RNAi-mediated abrogation of cathepsin B and MMP-9 gene expression in a malignant meningioma cell line leads to decreased tumor growth, invasion and angiogenesis. Int J Oncol 2007; 31: 1039-1050.
[34] Gocheva V, Wang HW, Gadea BB, Shree T, Hunter KE, Garfall AL, Berman T and Joyce JA. IL-4 induces cathepsin protease activity in tumor-associated macrophages to promote cancer growth and invasion. Genes Dev 2010; 24: 241-55.
[35] Zhu DM and Uckun FM. Cathepsin inhibition induces apoptotic death in human leukemia and lymphoma cells. Leuk Lymphoma 2000; 39: 343-354.
[36] Jung M, Lee J, Seo HY, Lim JS and Kim EK. Cathepsin inhibition-induced lysosomal dysfunction enhances pancreatic beta-cell apoptosis in high glucose. PLoS One 2015; 10: e0116972.
[37] Nalla AK, Gorantla B, Gondi CS, Lakka SS and Rao JS. Targeting MMP-9, uPAR, and cathepsin B inhibits invasion, migration and activates apoptosis in prostate cancer cells. Cancer Gene Ther 2010; 17: 599-613.
[38] Malla R, Gopinath S, Alapati K, Gondi CS, Gujrati M, Dinh DH, Mohanam S and Rao JS. Downregulation of uPAR and cathepsin B induces apoptosis via regulation of Bcl-2 and Bax and inhibition of the PI3K/Akt pathway in gliomas. PLoS One 2010; 5: e13731.